Properly Size Vents for Nonreactive and Reactive Chemicals

A simple, cost-effective approach to relief system sizing is outlined using DIERS-based calorimetry data for vapor, gassy, and hybrid systems. Easy-to-use screening guidelines are provided, eliminating the need for knowing thermophysical properties.

HANS K. FAUSKE,
FAUSKE & ASSOCIATES, INC.

Safe relief system designs require knowledge of chemical reaction rates, character, and energy release. The Design Institute for Emergency Relief Systems (DIERS) program *(1)*, sponsored by 29 companies under the auspices of AIChE, provided the chemical process industries (CPI) with the tools necessary to gather such data *(2, 3)*. A primary purpose of this effort was evaluation of emergency relief vent requirements, including energy and gas release rates for systems under upset conditions, and the effects of two-phase flow on the emergency discharge process.

These efforts resulted in what is now known as the DIERS methodology. This system for the design of pressure relief systems is widely acknowledged as state-of-the-art and is endorsed by the U.S. Occupational Safety and Health Administration and the U.S. Environmental Protection Agency as an example of good engineering practice.

It is frequently suggested, however, that the DIERS methodology can be so complex and time-consuming that it may be beyond the capability of many facility operators. Further, it has also been argued that this procedure can be overly conservative, leading to impractical relief system designs. These observations can be related to uncertainties or lack of knowledge of chemical kinetics, thermophysical properties, and relevant two-phase flow regimes.

Therefore, to ensure widespread and consistent use of the DIERS methodology, this article advances more user-friendly guidelines. These are benchmarked against available large-scale data to avoid uncertainties related to flow regimes and eliminate the need for thermophysical properties. The direct use of relevant data obtainable with the DIERS-based low-phi-factor calorimetry methodology eliminates the need for kinetic modeling (the thermal mass of the test cell is small with respect to the test sample).

DIERS calorimetry methodology

Typically, two approaches are used to obtain pressure relief requirements for chemical reactive systems depending on the strategy chosen for design *(4)*:

1. Computer simulation methods such as the DIERS-developed SAFIRE code *(5)* and Super Chems for DIERS *(6)*. The effective use of such simulation programs requires all basic physical, thermodynamic, and kinetic properties of the system.

2. Direct sizing from data of runaway calorimetry tests used in special-case venting models.

The requisite physical and kinetic data are

rarely available in the range of emergency relief conditions, and are time-consuming and costly to generate. Thus, the second approach is currently the most-frequently-used one, and is emphasized here, consistent with the need for more user-friendly techniques.

The three runaway reaction calorimeter devices in most general use are the Accelerating Rate Calorimeter (ARC), (Arthur D. Little), the DIERS bench-scale apparatus (Fauske & Associates's Vent Sizing Package (VSP)) and the Reactive System Screening Tool (RSST), also from our company *(4)*. The DIERS program produced the first and only existing adiabatic, sample thermal calorimeter by introducing automatic pressure tracking (APT), which allows a closed test cell phi-factor design approaching 1.0. This development, together with pioneering the need for low-phi-factor open test-cell designs and testing, facilitated, for the first time, safe, direct vent sizing from runaway reaction data without full-scale field verification *(2, 3)*. There are other adiabatic calorimeters similar to the DIERS bench-scale apparatus, such as the APTAC and PHI-TEC, but they are less commonly employed *(4)*.

Figure 1 shows the basic features of a typical DIERS bench-scale apparatus. This device was developed by DIERS to overcome data-acquisition limitations of the ARC for complex systems *(4)*. The unit illustrated here can be operated in either the closed or venting mode. The use of thin-wall metal test cells allows the data to be scaled up directly to plant size. APT controls the external pressure and prevents test cell rupture. In addition to closed-system operation that provides pressure/temperature data, the device can be used to check viscous behavior from venting tests, as well as provide information as to the system classification (*i.e.*, vapor, gassy, and hybrid reactions). In terms of vent sizing, this DIERS-based unit furnishes measured values of the self-heat rate and rate of pressure rise, which can be used to directly evaluate vapor or volumetric rates.

Figure 1. Basic functioning of a DIERS bench-scale calorimeter (VSP2) allows data to be scaled up directly for commercial-size equipment.

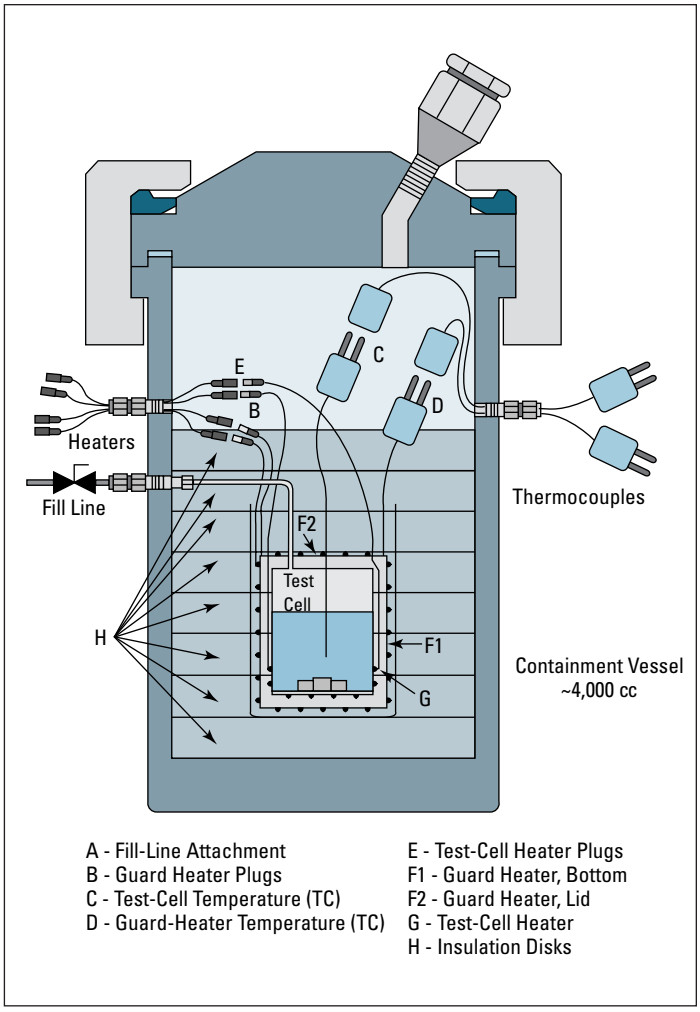

Other test apparatuses

Figure 2 shows another calorimeter that can quickly and safely determine potential chemical hazards and relevant vent sizing parameters *(3, 7)*. Basic components include a 10-mL open spherical glass test cell, its surrounding bottom-heater jacket and insulation, thermocouples and a pressure transducer, and a 350-cc stainless steel containment vessel that serves as both a pressure simulator and safety vessel. This device has a low, effective heat capacity relative to that of the sample, which may be expressed as a capacity ratio, or phi-factor, of approximately 1.04 (*i.e.*, quite adiabatic).

Heat loss from the test cell surface is compensated for by adding heat to the sample at a fixed rate (determined by precalibration). This device operates only in the venting mode and, therefore, provides information as to the system classification, *i.e.*, vapor, hybrid, and gassy reaction behavior. Closed-vessel data (such as equilibrium pressure over the sample) cannot be obtained, but the rates of self-heating and pressure rise are found, which can be used directly to evaluate vapor or gas volumetric rates. This device has temperature ramps to simulate fire exposure, a heat-wait-search mode of operation providing onset detection sensitivity as low as 0.1°C/min, and isothermal operation at elevated temperature. Endothermic

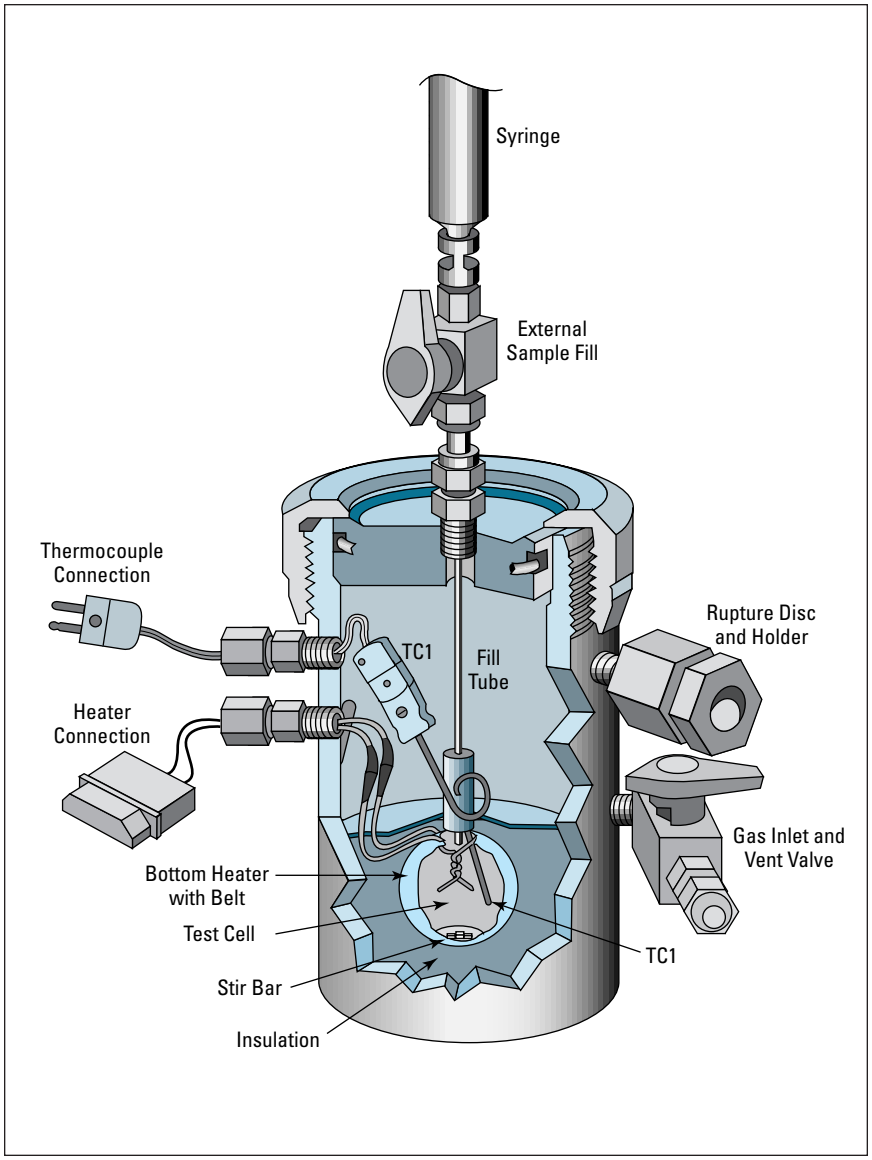

■ Figure 2. Operating in the venting mode, this calorimeter (RSST) determines the system classification, plus yield data for gas/vapor generation.

behavior (phase change) is also accommodated. (For recent improvements on this calorimeter, see Ref. 8.)

Flow regime characterization

Knowledge of the prevailing flow regime during emergency venting is essential to estimate a realistic, but safe, relief system design. Since it is not possible to predict the foaming behavior from physical properties alone, and since flow regime characterization methods for actual relief conditions are not available, the DIERS practice has usually been to design for "foamy" conditions, *i.e.*, homogeneous vessel situations, thus, erring on the safe side. Considering that the occurrence of foamy vs. nonfoamy conditions is sensitive to impurities, minute changes in concentration levels, etc., the flow regime characterization needs to be performed under actual runaway conditions coinciding with the relief venting process.

Tests can be run to distinguish between these two conditions (Figure 3). The device in Figure 3 (*8*) employs a small immersion heater and an attached thermocouple that is positioned in the upper freeboard space of the test cell. An auxiliary control box contains a dedicated power supply for the sensor. The detector temperature is displayed onscreen and is also logged to the output data file. Prior to externally heating the chemical sample itself, power is supplied to an internal heating coil to establish an elevated (base line) sensor temperature. This temperature should be well above the anticipated boiling (tempering) temperature of the sample. The detector operates on the simple principle that if the flow regime following the onset of boiling is foamy, then the detector will be wetted and rapidly cooled. If the flow regime is nonfoamy, then the detector thermocouple TC2 will continue to measure a temperature well in excess of the sample temperature TC1.

Figure 4 (*8*) shows an example of a typical test run for soapy water that was rapidly heated at about 30°C/min. When the sample temperature TC1 reached 100°C, the liquid foamed up, immediately quenching the detector and dropping its temperature TC2 to the sample boiling point. The profound difference in venting characteristics between nonfoamy and foamy systems are explained further below.

Nonreactive systems

Realistic sizing for fire emergencies for nonreactive systems requires information about the prevailing flow regime, *i.e.*, is the system in question nonfoamy or foamy following incipient boiling and vaporization? This is especially so for atmospheric storage tanks (3 oz.–2.5 psig design pressure) that are covered by API Standard 650, "Welded Steel Tanks for Oil Storage," 10th edition, API, Washington, DC (Oct. 1998). Relevant experimental data simulating

fire emergencies with nonfoamy (tap water) and foamy (1,000 ppm detergent in water) liquids *(9)* clearly illustrate the difference in venting behavior (see Figure 5). Note that the data obtained represent a scale up in volume of about 10^5 compared to that taken in the device in Figure 3, which illustrates similar trends, *i.e.*, the flow regime information from the bench-scale device can be applied to commerical-scale equipment.

Nonfoamy behavior — nonreactive systems

This venting requirement can be based upon all-vapor-venting consistent with the traditional approach *(10)*. The expected flow regime pattern is illustrated in Figure 5a, which results in a small liquid swell (typically less than 5%) due to the bubbles primarily forming and adhering close to the vertical walls *(9, 11)*. The minimum freeboard height h (m), below which two-phase venting can be expected (Figure 5a) is given by *(12)*:

$$h = \left(\frac{\dot{Q}}{2\pi U_E} \right)^{1/2} \qquad (1)$$

where U_E (m s^{-1}) is the Kutateladze *(13)* entrainment velocity given by:

$$U_E = 3\left[\frac{\sigma g \rho_l}{\rho_v^2} \right]^{1/4} \qquad (2)$$

where σ (kg s^{-2}) is the liquid surface tension, g (9.8 m s^{-2}) the gravitational constant, ρ_l (kg m^{-3}) the liquid density, and ρ_v (kg m^{-3}) the vapor density. $\dot{Q}$ (m^3 s^{-1}) is the volumetric vapor source resulting from the fire exposure and is given by:

$$\dot{Q} = \frac{Q_F}{\lambda \rho_v} \qquad (3)$$

where Q_F (J s^{-1}) is the total fire heat input rate (surface area × fire heat flux — see Ref. 10), and λ (J kg^{-1}) is the latent heat of vaporization. $\dot{Q}$ can also be represented in terms of the equivalent liquid volumetric heating rate, $\dot{T}$ (K s^{-1}), as follows:

$$\dot{Q} = \frac{V \rho_l c \dot{T}}{\lambda \rho_v} \qquad (4)$$

where V (m^3) is the volume of liquid, and c (J kg^{-1} K^{-1}) is the liquid specific heat. Considering vapor venting, the required vent area A (m^2) is given by:

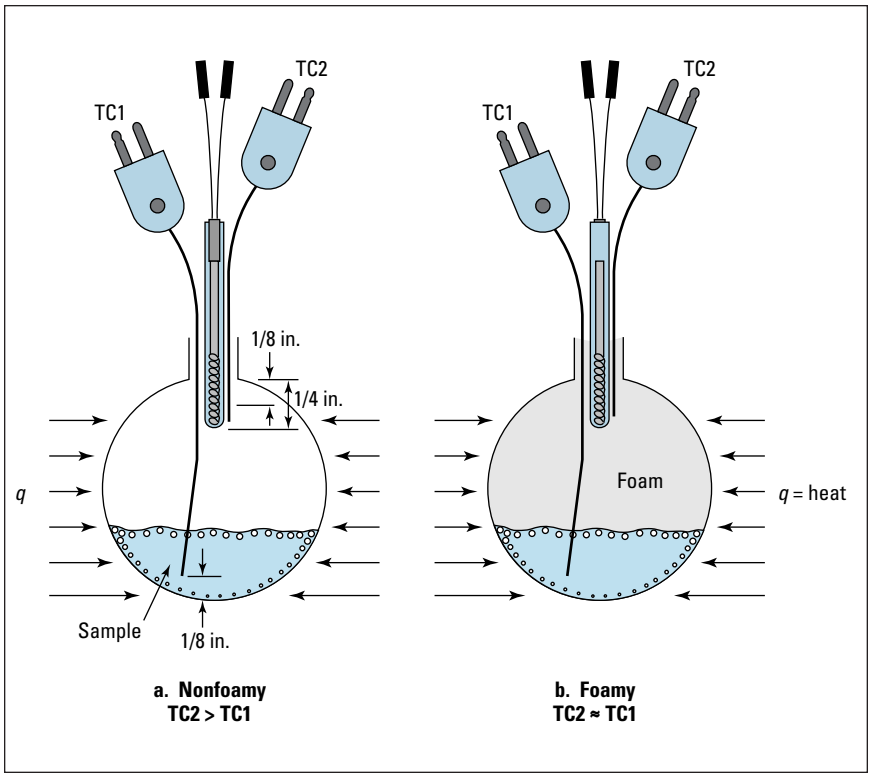

Figure 3. Tests can be run to see if a system is foamy or nonfoamy.

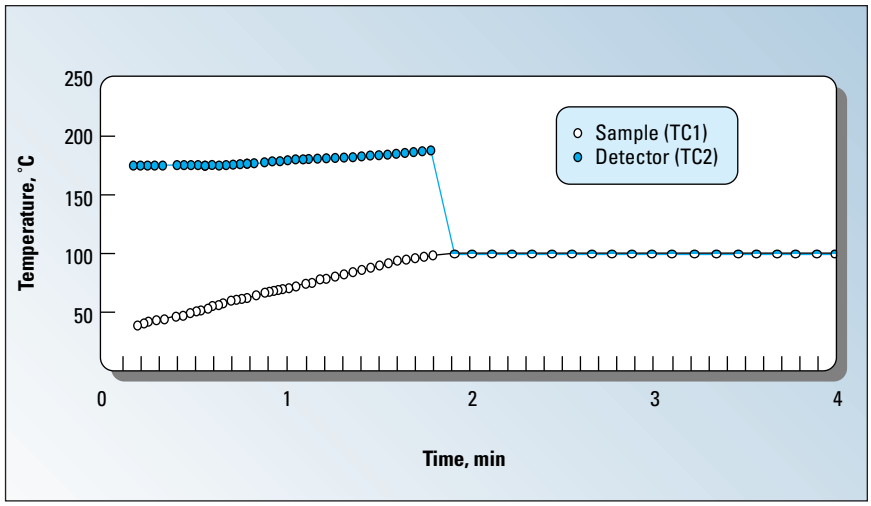

Figure 4. Foaming developed just under 2 min, dropping the temperature of the detector thermocouple TC2.

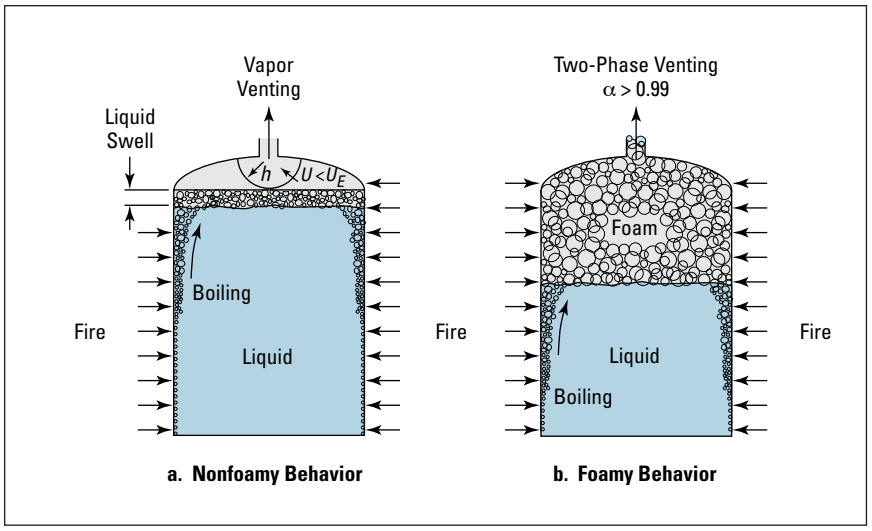

Figure 5. Nonfoamy and foamy venting behaviors for fire emergencies.

$$A = \frac{\dot{Q}}{C_D 0.61 \left(P/\rho_v\right)^{1/2}} \quad (5)$$

$$A = \frac{\dot{Q}}{C_D \left(2\Delta P/\rho_v\right)^{1/2}} \quad (6)$$

for critical and highly subcritical flow conditions, respectively. Here, C_D is the appropriate discharge coefficient, P (Pa) the venting pressure, and ΔP (Pa) the overpressure relative to the ambient pressure.

Vent area requirements predicted from Eqs. 5 and 6 are compared to available large-scale nonfoamy data in Table 1. The atmospheric water data were obtained with sharp-entrance short-vent ducts, *i.e.*, the appropriate value of C_D = 0.61. The noted good agreement is consistent with a freeboard value of less than 5%, which accommodates both the liquid swell and the absence of liquid entrainment according to Eq. 1.

We note that, for the propane trial listed in Table 1 *(14)*, Eq. 5 predicts a somewhat larger vent area requirement. This is consistent with the stated overpressure ΔP = 40 psi. Also, the listed propane trial, despite the presence of adequate pressure relief, experienced a catastrophic failure, *i.e.*, a so-called BLEVE (boiling liquid expanding vapor explosion). The occurrence of BLEVEs with tanks filled with pressure-liquefied gas (PLG) mostly involve fire impingement, ranging from partial or complete fire engulfment to local jet or torch fires. Fire exposure leads to high wall-temperatures above the liquid level and to material weakening. Catastrophic tank failure may result, even though the relief valve is open and is venting vapor at a rapid rate. The sudden release and explosive evaporation of a superheated liquid can lead to severe consequences. If tanks can empty before they can fail, BLEVEs are eliminated and the outcomes will be much less hazardous.

Timely removal of PLG can be facilitated by installing a dip-tube relief system in addition to the traditional

Table 1. Fire simulation experiments and model predictions.

System	$(A/V)_{exp}$, m^{-1}	P, psia	ΔP, psi	$\dot{T}$, °C min^{-1}	$(A/V)_{predictions}$, m^{-1}	
					Foamy	Vapor Venting
Water, 0.312 m^3 Nonfoamy	1.62×10^{-3}	14.7	~ 0.7	2.5	—	1.68×10^{-3} (Eq. 6)
Water, 0.312 m^3 Foamy	6.48×10^{-3}	14.7	~ 0.4	2.5	(5.83×10^{-2})* 8.86×10^{-3} (Eq. 6)	—
Propane, 122 m^3 Nonfoamy	4.15×10^{-5}	285	40	3.36	—	4.80×10^{-5} (Eq. 5)

* DIERS Methodology, Refs. 15 and 16.

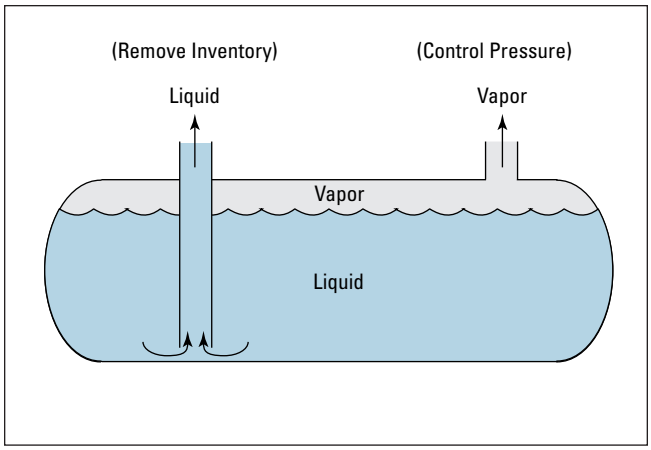

Figure 6. Combined liquid and vapor venting is used to help prevent BLEVEs.

vapor relief system (Figure 6). The latter controls the pressure by providing adequate vapor venting, while the dip-tube provides rapid liquid removal, which can largely empty the tank before reaching rupture. Accounting for inherent temperature stratification (*i.e.*, subcooled liquid), and time to failure in connection with both fire engulfment and torch fire, indicates that installing a liquid removal system of similar size to the vapor relief system will empty the tank before failure can occur, *i.e.*, prevent most BLEVEs.

Foamy behavior — nonreactive systems

In contrast to nonfoamy behavior, for foamy systems, such as exemplified by the foamy water trial listed in Table 1, a very high void fraction regime ($\alpha > 0.99$) continues to enter the vent line until the vessel is nearly empty, *i.e.*, a freeboard volume free of liquid is only established after a large fraction of the liquid has vented. Also, note that during the two-phase venting, the vapor volumetric rate remains invariant due to the constant heat input. The implication of this behavior leads to a larger vent area, but also largely eliminates the potential for a BLEVE, as the walls continue to be wetted until most of the liquid has been vented (Figure 5b).

As for the increased vent area requirement, we note that the proposed DIERS methodology considering uniform bubbly flow behavior *(15, 16)* grossly overpredicts the requirement by an order of magnitude, as illustrated in Table 1. Replacing the vapor density ρ_v in Eq. 6 with the two-phase density $\rho_l (1 - \alpha) + \rho_v \alpha$, and setting $\alpha = 0.99$, a reasonably safe vent area is estimated, as shown in Table 1. Matching the experimental vent area with the measured overpressure of 0.4 psi results in $\alpha = 0.995$.

Given the high value of the foam void fraction, a similar approach can be used for critical flow conditions, with $\rho_l (1 - \alpha) + \rho_g \alpha$ replacing ρ_v in Eq. 5 with $\alpha = 0.99$. Additional experiments to confirm the general use of this approach appear warranted.

Finally, in the case of fire exposure to vessel jackets containing liquids, two-phase venting needs to be considered regardless of the classification of the flow regime. For such conditions, the wall boiling boundary layer *(11)* takes on the dimension of the narrow jacket channels, resulting in essentially a uniform void distribution. In the case of nonfoamy and foamy liquids, the DIERS churn-turbulent and bubble-flow methodologies are directly applicable *(17, 18)*. As such, note that the required vent areas for the vessel jackets may be larger than those allotted for the vessel itself, since for externally heated vessels, the vent area is proportional to the heat-transfer area and not the vessel volume *(15)*.

Reactive systems

Following the AIChE DIERS methodology, three types of reactive systems are usually distinguished for venting character including vapor, gassy, and hybrid (Figure 7). The venting character and corresponding relief area requirement are easily determined using the DIERS calorimetry methodology.

For the **vapor system** (*i.e.*, total pressure is equal to the vapor pressure), the principal parameter determining the vent size requirement is the rate of temperature rise $\dot{T}$ (°C min^{-1}), measured at the relief set pressure P (psia). Since, for the vapor system, the reaction is entirely tempered by the latent heat of vaporization, the lowest practical relief set pressure (*i.e.*, that well below the maximum allowable pressure) results in the smallest relief area requirement.

For the **gassy system,** in the absence of any tempering (*i.e.*, the total pressure is equal to the noncondensible gas pressure), the principal parameter determining the vent size requirement is the measured maximum rate of pressure rise $\dot{P}_{Max}$ (psi min^{-1}). In this case, the smallest vent size requirement is obtained by considering the maximum allowable pressure P (psia).

For the **hybrid system,** with both gas production and vaporization occurring simultaneously (*i.e.*, the total pressure is equal to the sum of the gas partial pressure and the vapor pressure), both the rate of temperature rise $\dot{T}$ (°C min^{-1}), and the rate of pressure rise $\dot{P}$ (psi min^{-1}) are needed to determine the proper vent size for a specified venting pressure.

Hybrid system vent sizing

If a detailed kinetic model is not readily available, which is often the case, the measured self-heat rate $\dot{T}$ (K s^{-1}), and the rate of pressure rise $\dot{P}$ (Pa s^{-1}) for a given relief set pressure P (Pa) using DIERS-based calorimetry, can be applied directly to assess the volumetric rates of vapor

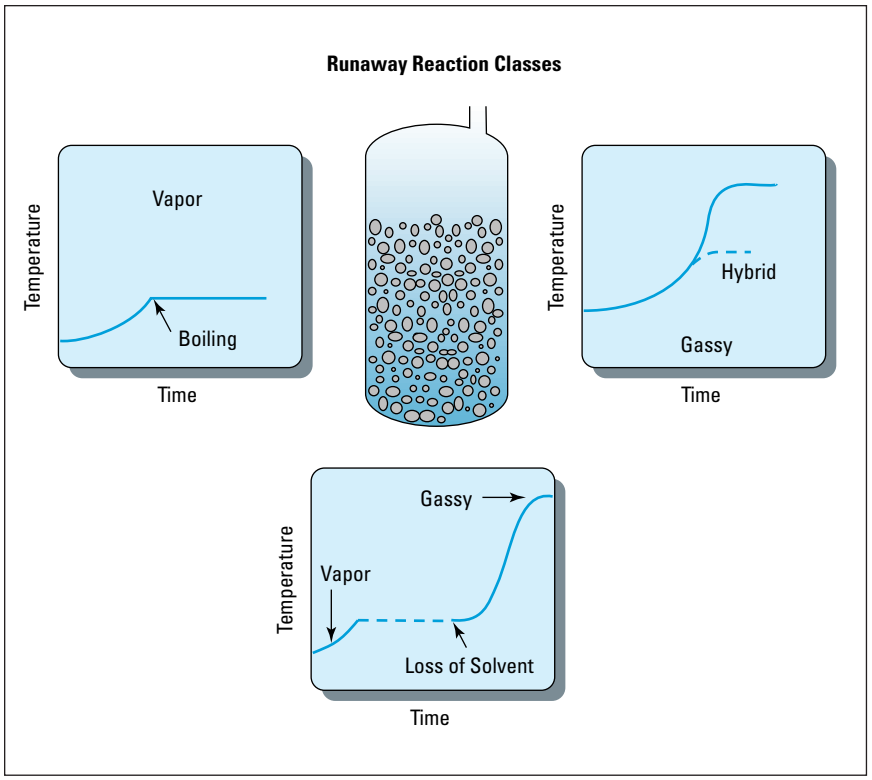

Figure 7. DIERS methodology considers three types of runaway reactions.

$\dot{Q}_v$ ($m^3\ s^{-1}$) and gas $\dot{Q}_g$ ($m^3\ s^{-1}$):

$$\dot{Q}_v = \frac{mcT}{\lambda \rho_v} \tag{7}$$

$$\dot{Q}_g = \frac{mv}{m_t}\frac{\dot{P}}{P} \tag{8}$$

where m (kg) is the reactant mass, m_t (kg) the test sample mass, and v (m^3) the test freeboard volume.

The validity of the above equations has been demonstrated with calorimetry data (m_t = 0.01 kg and v = 3.5 × 10^{-4} m^3) obtained with H_2O_2 solutions (25 wt. % in H_2O), where kinetics and physical properties are well known from RSST tests *(19)*. As illustrated in Figure 8 (some of the values are from Ref. 20), the data for H_2O_2 results in $\dot{T}/\dot{P} \approx 4$, which is invariant with H_2O_2 and catalyst concentrations. The high-pressure test (where vapor stripping is suppressed) clearly shows that the system produces noncondensible gas with the rate of pressure rise $\dot{P} >> 0$. The low-pressure run also clearly illustrates that the reaction is tempered, since the rate of temperature rise $\dot{T} \rightarrow 0$, as the temperature approaches 100°C. The corresponding rates of temperature and pressure changes are obtained from the high-pressure test and are about 4°C min^{-1} and 1 psi min^{-1}, respectively.

Considering gas-vapor venting only, the vent area to volume ratio A/V (m^{-1}) can be estimated from Eqs. 9 and 10 (see box below):

$$A/V = \frac{1}{0.61 C_D}\left[\frac{\rho c \dot{T}}{\lambda P}\left(\frac{RT}{M_{w,v}}\right)^{1/2} + \frac{\rho v \dot{P}}{m_t P}\left(\frac{M_{w,g}}{RT}\right)^{1/2}\right] \tag{9}$$

for critical and highly subcritical flow conditions, respectively, where ρ (kg m^{-3}) is the loading density, T (K) the temperature, R (8,314 Pa-m^3/K-kg mole) the gas constant, P_b (Pa) the back pressure, $M_{w,v}$ the vapor molecular weight, and $M_{w,g}$ the gas molecular weight.

The above vent sizing methodology for hybrid systems is consistent with the large-scale 200-kg 50 wt. % H_2O_2 runaway reaction trials reported by Wilberforce *(20)*, as illustrated in Table 2. Measured self-heat rates reported for Trials 3 and 4 are illustrated in Figure 8 (the dashed portions of the curves represent extrapolations to tempering conditions of 106°C and 130°C, corresponding to measured overpressures of 0.9 psi and 40 psi, respectively). The reported absence of two-phase flows as the tempering is approached for test Trial 3 is another example of the flow regime complexity during venting conditions. The absence of liquid ejection suggests that the vapor/gas release is highly nonuniform, due to inherent nonequilibrium conditions with the majority of the release occurring at the walls and free liquid surface, resulting in insignificant liquid swell in the absence of foamy conditions, similar to that illustrated in Figure 5a.

Given a freeboard volume of about 10% after accounting for the liquid swell, the absence of two-phase venting is also consistent with the entrain-

$$A/V = \frac{1}{C_D}\left[\frac{\rho c \dot{T}}{\lambda P}\left(\frac{RT}{M_{w,v}}\right)^{1/2} + \frac{\rho v \dot{P}}{m_t P}\left(\frac{M_{w,g}}{RT}\right)^{1/2}\right]\left[\frac{1}{2\left(1 - P_b/P\right)}\right]^{1/2} \tag{10}$$

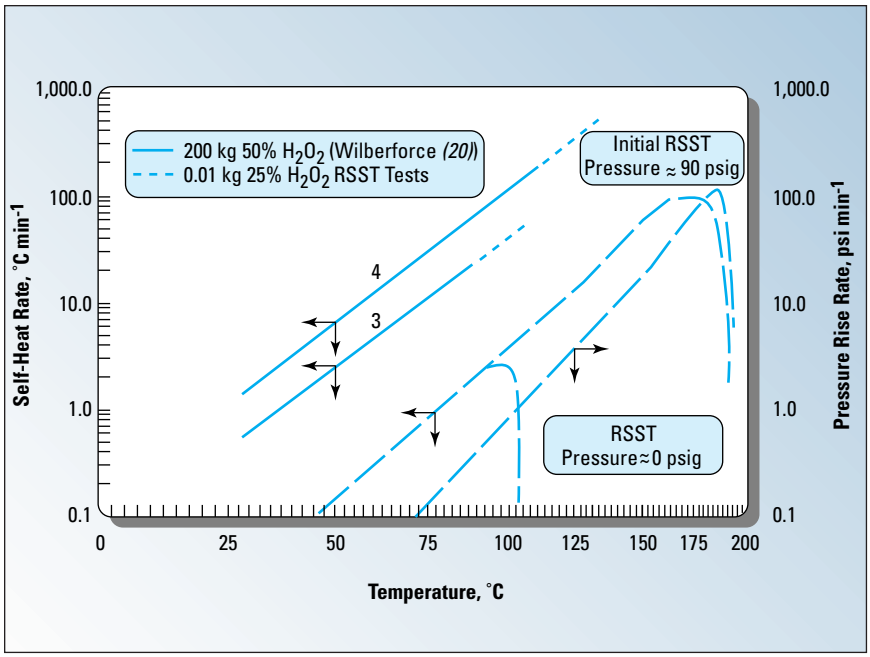

Figure 8. Calorimetric data for two systems of H_2O_2/H_2O under varying conditions.

ment consideration given by Eq. 1. The absence of two-phase venting is further confirmed by the estimated vent area based upon all vapor/gas venting from Eq. 10 (using the measured overpressure of 0.9 psi along with the measured self-heat rate of 55°C min^{-1} and a pressure rise rate of 14 psi min^{-1}, based upon the noted calorimetric information $\dot{T}/\dot{P} \sim 4$, which is in good agreement with the available vent area (see Table 2).

Trial 4 in Table 2, with a higher catalyst concentration and a smaller available vent area, resulted in rapid pressurization and catastrophic vessel failure as the overpressure reached about 40 psi. This is not surprising, considering that the vent area estimated from Eq. 9 (using the noted overpressure and the temperature and pressure rise rates) results in a value well above the available vent area (see Table 2). The lesson to be learned here is to never design a vent area that is less than that required by all vapor/gas venting.

As noted by Wilberforce *(20)*, the absence of liquid ejection as tempering is approached for test Trial 3 is seriously at odds with the often used DIERS two-phase flow methodology, which considers homogeneous vessel conditions with initiation of two-phase venting as the runaway reaction becomes tempered *(21, 22)*. However, should a flow regime prevail (nonfoamy or foamy) that will result in uniform void distribution and two-phase venting, consideration of mass loss of reactants due to gas generation before reaching reaction tempering, in addition to allowance of modest overpressures (30–40%), indicates vent areas compatible with predictions from Eqs. 9 and 10.

The lesson to be learned here is that the possible early mass loss effect (illustrated later for gassy systems) and the overpressure effect (discussed below for vapor systems) eliminate the need to consider uncertainties related to flow regimes and nonequilibrium effects, with the minimum vent area determined by considering only vapor/gas venting. Note, however, for effluent system design, the possibility of two-phase venting should be accounted for even if it is not the basis for the vent design.

Vapor system vent sizing

The principal quantity of interest is the reaction self heat rate $\dot{T}$ (K s^{-1}) at the relief set pressure P (Pa) and temperature T (K); then Eqs. 9 and 10 reduce to:

$$A/V = \frac{1}{0.61 C_D} \frac{\rho c \dot{T}}{\lambda P} \left(\frac{RT}{M_{w,v}} \right)^{1/2} \qquad (11)$$

Table 2. Representative 200 kg, 50 wt. % H_2O_2 tests and comparison with models.

Trial No.	$(A/V)_{exp.}$, m^{-1}	P, psia	ΔP, psi	$\dot{T}$, °C min^{-1}	$\dot{P}$, psi min^{-1}	$(A/V)_{predictions}$, m^{-1} DIERS Two-Phase	$(A/V)_{predictions}$, m^{-1} Vapor/Gas Venting
3	2.59×10^{-2}	14.7	~ 0.9	55	14	2.50×10^{-1}	2.85×10^{-2}
4	1.15×10^{-2}	14.7	> 40	500	125	—	3.40×10^{-2}

$$A/V = \frac{1}{C_D}\frac{\rho c \dot{T}}{\lambda P}\left(\frac{RT}{2\left(1-P_b/P\right)M_{w,v}}\right)^{1/2} \quad (12)$$

for critical and highly subcritical flow conditions, respectively.

Representative data from the DIERS Phase II Large-Scale Integral Tests *(23)* consisting of a series of styrene polymerization in ethylbenzene solvent are listed in Table 3. Initial conditions at the beginning of venting, as well as the observed overpressures ΔP are noted. The DIERS data clearly demonstrate:

1. The presence of liquid swell and two-phase venting;

2. The importance of allowing for modest overpressures in drastically reducing the vent size requirements; and

3. The complexity related to the prevailing flow regime during the venting process.

Best-fit interpretation of measured integral pressure/time and average vessel void-fraction-time data following incipient venting suggests a churn-turbulent or nonfoamy vessel hydrodynamic behavior for Trial ICRE (Integral Chemical Reacting Experiments) 2000-5 with its higher concentration of polystyrene, while a bubbly-flow or foamy-like behavior is suggested for Trial ICRE 32-9 *(1, 5)*. This difference in the vapor disengagement behavior shows up principally in the considerably higher overpressure noted in Trial ICRE 32.9, despite the smaller value of L/D = 16 (C_D = 0.95), as compared to 340 (C_D = 0.5) for Trial ICRE 2000-5. It is not possible at present to predict this behavior without testing. In the absence of flow-regime test data under prototypic emergency relief conditions, the DIERS methodology recommends the use of the conservative bubbly or homogeneous two-phase vessel models.

A vent area requirement based upon all vapor venting (Eq. 11) appears adequate.

Typical predictions from two-phase venting models (Huff *(24)*, Leung *(16)*, and Fauske *(25)*) using the measured overpressures are illustrated in Table 3. For Trial ICRE 32-9, the models are based upon homogeneous vessel behavior, while for Trial ICRE 2000-5, both homogeneous and churn-turbulent (the numbers in parentheses) predictions are provided.

The simple screening model provided by Fauske (limited to overpressures of 10–40% of the absolute relief pressure) is easy to use, as it requires essentially no information about physical properties, the only key information needed being the self-heat rate at the relief set pressure. The Leung treatment *(16, 18)* represents the more rigorous model, and is the preferred method for design purposes *(4)*. Using the initial conditions for Trial ICRE 32-9 and considering 0% overpressure, the Leung model predicts a value of $A/V = 3.9 \times 10^{-2}$ m^{-1}, illustrating the importance of allowing for overpressure in designing reasonable vent requirements for vapor-like systems. As such, a most interesting observation, related to the overpressure effect in reducing the vent size, is that a vent area requirement based upon all vapor venting (Eq. 11) appears adequate as illustrated in the righthand column of Table 3.

Further illustration of the overpressure effect is illustrated in Figures 9 and 10.

Table 3. Representative DIERS reaction tests and comparison with models.

Test	$(A/V)_{exp.}$, m^{-1}	P, Pa	T, K	ΔP, Pa	$\dot{T}$, °C s^{-1}	$(A/V)_{prediction}$, m^{-1} Ref. 24	Ref. 16	Ref. 25	Vapor Venting
ICRE 32-9* 0.32 m^3	1.92×10^{-3} (C_D ~ 0.95)	5.15×10^5	485	1.80×10^5	0.395	2.55×10^{-3}	2.60×10^{-3}	1.85×10^{-3}	1.82×10^{-3} Eq. 11
ICRE 2000-5† 2.19 m^3	2.26×10^{-3} (C_D ~ 0.5)	5.45×10^5	492	1.25×10^5	0.36	6.10×10^{-3}	6.30×10^{-3} (3.40×10^{-3})	4.60×10^{-3} (2.30×10^{-3})	2.40×10^{-3} Eq. 11

* 20% Ethylbenzene/61% styrene/19% polystyrene.
† 15% Ethylbenzene/50% styrene/35% polystyrene.

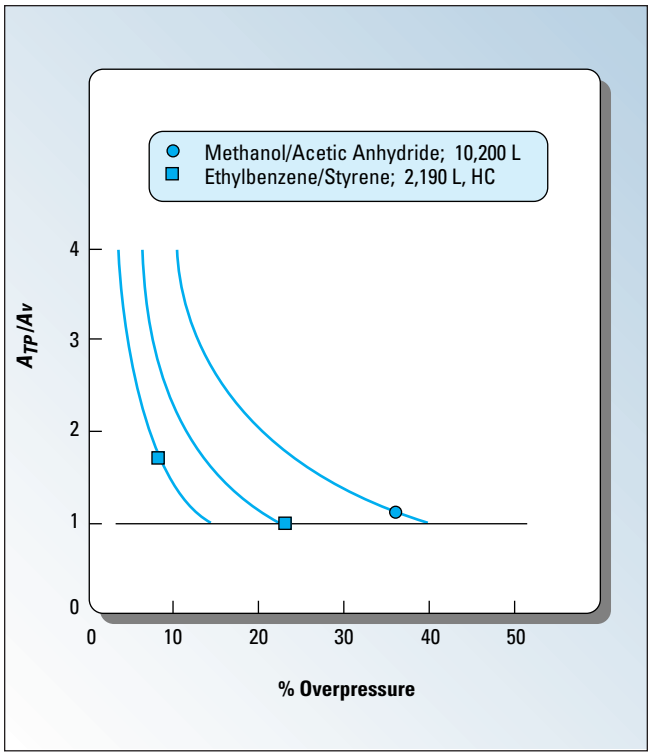

Figure 9. Nonfoamy data (A_{TP}) and comparison with all-vapor venting (A_v).

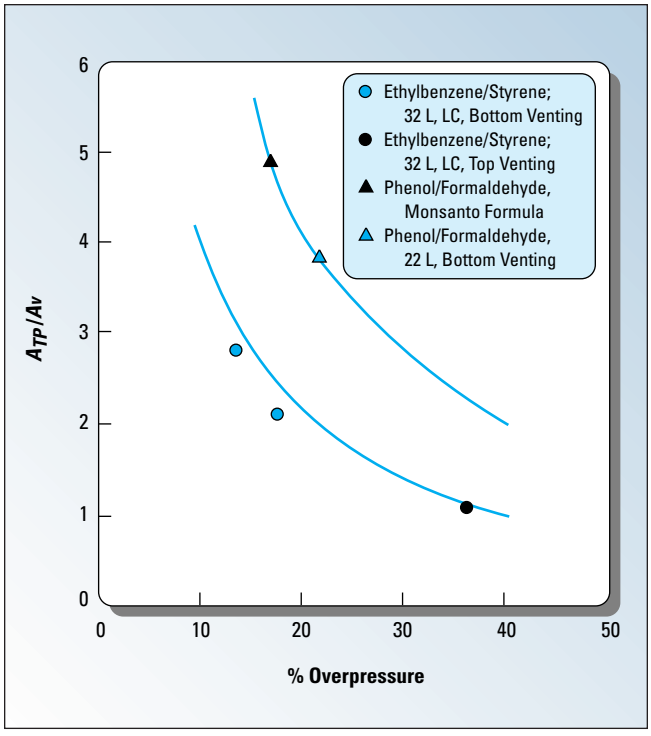

Figure 10. Foamy and bubbly-like data (A_{TP}) and comparison with all-vapor venting (A_v).

Vent areas A_{TP} from available large-scale reaction experiments with nonfoamy or churn-turbulent -like systems (10 m^3 methanol/acetic anhydride) *(26)*, and the DIERS 2 m^3 high-conversion (HC) ethylbenzene/styrene *(1)*, ratioed to the corresponding all-vapor venting areas A_v estimated from Eq. 11, are illustrated in Figure 9. Both two-phase flow theory *(25)* indicated by the solid lines and the data points show that, for nonfoamy systems and allowance of modest overpressure, the required vent area can be assessed considering vapor venting only, *i.e.*, Eq. 11.

The vent sizing formula, A (in.^{2}) = 0.053V (gal), based upon large-scale experience and used for phenolic resins reactors *(27)*, is used to illustrate the overpressure effect on venting requirements in Figure 10 for foamy or bubbly-like systems. Noting that the Monsanto formula is based upon a P value of about 1.5 psig and a $\dot{T}$ value of about 6.5°C min^{-1}, we estimate that the formula represents an overpressure of about 16%. At this percentage, the value of A_{TP}/A_v is about 4.9 (see Figure 10). (For a P_s of 1.5 psig and zero overpressure, this ratio would be about 160 based upon a flashing two-phase flow condition.)

The noted overpressure of 16% and the solid curve representing the overpressure effect are obtained by combining the Monsanto formula with the homogeneous vessel and vent flow formula: $A_{TP} = m\ \dot{T}\ /2 \times (T/c)^{1/2}\ \Delta P$, where ΔP (Pa) is the overpressure *(25)*. The latter formula is in good agreement with the low-conversion (LC) ethylbenzene/styrene data *(1)* exhibiting bubbly-like behavior, as indicated in Table 3 and further illustrated in Figure 10. The interpretation of the Monsanto formula is also in excellent agreement with recent 22-L bottom-vented phenol/formaldehyde tests *(28)*. For a measured overpressure of 21.7%, the value of A_{TP}/A_v is about 3.8 (see Figure 10).

Considering the enveloping nature of the phenol/formaldehyde system with its water-like properties, both theory and large-scale experience suggest that, for foamy systems and allowance of modest overpressure of about 40%, an adequate vent size can be based upon twice the area estimated for all-vapor venting (see Figure 10). This observation will be used later in this article when easy-to-use

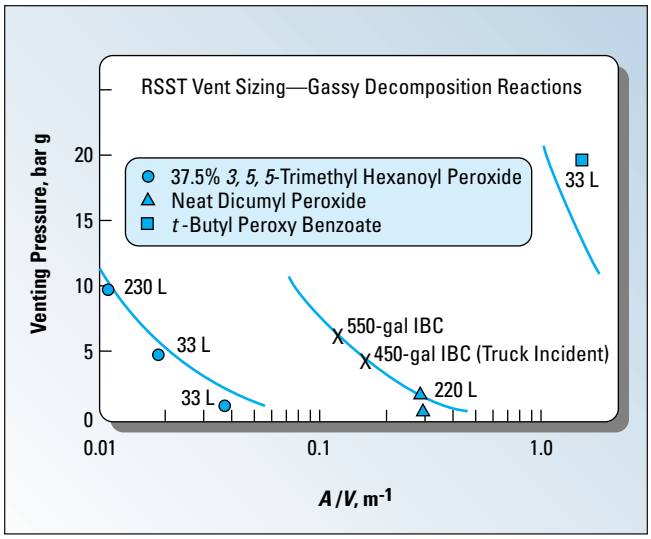

Figure 11. Large-scale runaway peroxide decomposition data and comparison with calorimetric simulation with all-gas venting (Eq. 13).

Table 4. Application of Eqs. 14 and 15.

System	C		$\dot{T}_i$	$\dot{P}$
Vapor, Foamy	7×10^{-3}	{8×10^{-4}}*	$\dot{T}(P)$	0
Vapor, Nonfoamy	3.5×10^{-3}	{4×10^{-4}}*	$\dot{T}(P)$	0
Hybrid	3.5×10^{-3}	{4×10^{-4}}*	$\dot{T}(P)$	$\dot{P}(P)$
Gassy	3.5×10^{-3}	{4×10^{-4}}*	0	$\dot{P}_{Max}$

* { } represents highly subcritical flow.

screening guidelines are presented for reactive systems.

Gassy system vent sizing

For these systems, Eq. 9 reduces to:

$$A/V = \frac{1}{0.61 C_D} \frac{\rho v \dot{P}}{m_t P} \left(\frac{M_{w,g}}{RT} \right)^{1/2} \quad (13)$$

and the maximum rate of pressure rise $\dot{P}$ is of principal interest.

Available venting data for peroxide systems, 37.5 wt. % *3,5,5*-trimethyl hexanoyl peroxide *(29)*, neat dicumyl peroxide *(30)*, and *t*-butyl peroxy benzoate *(29)* are compared to predictions from Eq. 13 in Figure 11, illustrating good agreement with both low, intermediate, and high peroxide energetics-levels. The calorimetric measured peak $\dot{P}$ values for these systems ($m_t \approx$ 0.01 kg) are 1,000, 4,000, and 100,000 psi min^{-1} for 37.5 wt. % *3,5,5*-trimethyl hexanoyl peroxide, neat dicumyl peroxide, and *t*-butyl peroxy benzoate, respectively *(19)*. The predictions for neat dicumyl peroxide are also consistent with incident data reported by Gove *(30)*.

The DIERS methodology for gassy systems *(21)*, considering initiation of two-phase flow at the measured peak reactive conditions and no prior material loss, overestimates the vent areas shown in Figure 11 by at least an order of magnitude. As indicated by the calorimetric tests, significant material losses occur well before reaching peak reactive conditions, further justifying the assumption of gas venting only. In addition, there is a transition from a homogeneous to propagating-reaction behavior as the peroxide energetics-level increases *(19, 31)*. Such transitions strongly influence the peak-volumetric gas-generation rate and require experimental determination, as provided by the DIERS-based calorimetry. The transition, as well as the rate of propagation, cannot be predicted by theoretical means.

Screening design guidelines

Based upon the above experience with reactive systems, the following simple formulas can be used to easily guide the relief requirements for

Table 5. Available large-scale experimental and screening guideline predictions.

System	$(A/V)_{exp.}$, m^{-1}	P_i, psia	ΔP_i, psi	$\dot{T}_i$, °C min^{-1}	$\dot{P}_i$, psi min^{-1}	A/V Screening Guidelines
Hybrid: 50% H_2O_2, 0.22 m^3	2.59×10^{-2}	14.7	~ 1	55	14	2.76×10^{-2}
Gassy: Dicumyl Peroxide, 0.22 m^3	2.8×10^{-1}	44	—	—	4,000	3.18×10^{-1}
Vapor: Phenol/Formaldehyde, 19 L	2.94×10^{-2}	27.7	4.5	62	—	3.13×10^{-2}
Vapor: Ethylbenzene/Styrene, 32 L	1.92×10^{-3}	75	27	23.7	—	2.30×10^{-3}
Vapor: Ethylbenzene/Styrene, 2.19 m^3	2.26×10^{-3}	79	18	21.6	—	2.17×10^{-3}
Vapor: Methanol/Acetic Anhydride, 10.2 m^3	2.21×10^{-3}	105	38	75	—	2.5×10^{-3}
Vapor: Isopropanol/Propionic Anhydride, 0.34 m^3	2.17×10^{-2}	21.9	14.9	80	—	2.46×10^{-2}

vapor, gassy, and hybrid systems:

$$A/V = \frac{C}{C_D P}\left(\dot{T} + \dot{P}\right) \quad (14)$$

$$A/V = \frac{C}{C_D \Delta P^{1/2}}\left(\dot{T} + \dot{P}\right) \quad (15)$$

for critical and highly subcritical flow conditions, respectively, where A (m^2) is the vent area, V (m^3) the volume of reactants, $\dot{T}$ (°C /min^{-1}) is the rate of temperature rise, $\dot{P}$ (psi min^{-1}) the rate of pressure rise, P (psia) the venting pressure in case of critical flow, and ΔP (psi) the available pressure drop in case of highly subcritical flows.

Values of C and the application of Eqs. 14 and 15 are provided in Table 4. C_D is a flow reduction factor (L/D = 0, C_D ~ 1.0; L/D = 50, C_D ~ 0.75;

Literature Cited

1. **Fisher, H. G., *et al.*,** "Emergency Relief System Design Using DIERS Technology," AIChE, New York (1992).
2. **Fauske, H. K., and J. C. Leung,** "New Experimental Techniques for Characterizing Runaway Chemical Reactions," *Chem. Eng. Progress,* **81**(8), pp. 39–46 (Aug. 1985).
3. **Creed, M. J., and H. K. Fauske,** "An Easy, Inexpensive Approach to the DIERS Procedure," *Chem. Eng. Progress,* **86** (3), pp. 45–49 (Mar. 1990).
4. **Center for Chemical Process Safety,** "Guidelines for Pressure Relief and Effluent Handling Systems," CCPS, AIChE, New York (1998).
5. **Grolmes, M. A., and J. C. Leung,** "Code Method for Evaluating Integrated Relief Phenomena," *Chem. Eng. Progress*, **81** (8), pp. 47–52 (Aug. 1985).
6. **Melham, G. A., and H. G. Fisher**, "An Overview of Super Chems for DIERS for Emergency Relief System and Effluent Handling Designs," *Process Safety Progress,* **16** (3), pp. 185–201 (Fall 1997).
7. **Fauske, H. K.,** "Reactive System Screening Tool," U.S. Patent No. 5,229,074 (July 20, 1993).
8. **Burelbach, J. P.,** "Advanced Reactive System Screening Tool (ARSST)," *Proc. Beyond Regulatory Compliance: Making Safety Second Nature*, Mary Kay O'Connor Process Safety Center Symposium, College Station, TX (Oct. 26–27, 1999).
9. **Fauske, H. K., *et al.*,** "Emergency Relief Vent Sizing for Fire Emergencies Involving Liquid-Filled Atmospheric Storage Vessels," *Plant/Operations Progress,* **5** (4), p. 205 (1986).
10. **Crozier, R. A.,** "Sizing Relief Valves for Fire Emergencies," *Chem. Eng.,* **81** (10), p. 49 (Oct. 28, 1985).
11. **Grolmes, M. A., and M. Epstein,** "Vapor-Liquid Disengagement in Atmospheric Liquid Storage Vessels Subjected to External Heat Source," *Plant/Operations Progress,* **4** (4), pp. 200–206 (Oct. 1985).
12. **Epstein, M., *et al.*,** "The Onset of Two-Phase Venting via Entrainment in Liquid-Filled Storage Vessels Exposed to Fire," *J. Loss Prev. Process Ind.,* **2** (1), p. 45 (1989).
13. **Kutateladze, S. S.,** "Elements of the Hydrodynamics of Gas-Liquid Systems," *Fluid Mechanics - Soviet Research,* **1,** p. 29 (1972).
14. **U.S. Dept. of Transportation,** "Final Report FRA-ORRD75-32," U.S. DOT (1984).
15. **Fisher, H. G., and H. S. Forrest,** "Protection of Storage Tanks From Two-Phase Flow due to Fire Exposure," *Process Safety Progress*, **14** (3), pp.183-199 (July 1995).
16. **Leung, J. C.,** "Simplified Vent Sizing Equations for Emergency Relief Requirements in Reactors and Storage Vessels," *AIChE J.*, **32** (10), pp. 1622–1634 (1986).
17. **Leung, J. C.,** "Overpressure During Emergency Relief Venting in Bubbly and Churn-Turbulent Flow," *AIChE J.*, **33** (6), pp. 952–958 (1987).
18. **Fauske & Associates, Inc.,** "Vent Sizing Software Program (VSSP)," Fauske, Burr Ridge, IL (updated version 2.1, 1995).
19. **Fauske, H. K.,** "The Reactive System Screening Tool (RSST): An Easy, Inexpensive Approach to the DIERS Procedure," *Proc. Int. Symp. on Runaway Reactions, Pressure Relief Design, and Effluent Handling*, New Orleans (Mar. 11–13, 1998).
20. **Wilberforce, J. K.,** "Emergency Venting of Hydrogen Peroxide Tanks," CEFIC Hydrogen Peroxide Safety Conference, Gotherburg, Sweden (Sept. 22, 1988).
21. **Leung, J. C., and H. K. Fauske,** "Runaway System Characterization and Vent Sizing Based on DIERS Methodology," *Plant/Operation Progress*, **6** (2), p. 77 (1987).
22. **Leung, J. C.,** "Venting of Runaway Reactions with Gas Generation," *AIChE J.*, **38** (5), pp. 723–733 (1992).
23. **Grolmes, M. A., *et al.*,** "Large-Scale Experiments of Emergency Relief Systems," *Chem. Eng. Progress,* **81**(8), pp. 57–62 (Aug. 1985).
24. **Huff, J. E.,** "Emergency Venting Requirements," *Plant/Operations Progress,* **1** (4), pp. 211–229 (1982).
25. **Fauske, H. K.,** "Emergency Relief System Design for Runaway Chemical Reaction: Extension of DIERS Methodology," *Chem. Eng. Res. Des.,* **67,** pp. 199–202 (Mar. 1989).
26. **Linga, H., *et al.*,** "Large-Scale Runaway Reaction Tests," paper presented at the Loss Prevention Symposium, AIChE Spring National Meeting, New Orleans (Mar. 8–12, 1998).
27. **Howard, W. B.,** "Reactor Relief Systems for Phenolic Resins," internal memo, Monsanto Co., St. Louis (June 1973).
28. **Leung, J. C., *et al.*,** "Phenolic Runaway Reaction — Pressure Relief and Containment," *Proc. Int. Symp. on Runaway Reaction, Pressure Relief Design, and Effluent Handling*, New Orleans (Mar. 11–13, 1998).
29. **Wakker, J. P., and J. J. deGroot,** "Venting of Decompositions of Energetic Liquids Using a Bottom Vent," *Proc. of Process Plant Safety Symposium*, Vol. 2, pp. 55–71, Houston (1996).
30. **Gove, S. H.**, "Emergency Pressure Relief for Intermediate Bulk Containers Containing Dicumyl Peroxide," DIERS User Group Meeting, Houston (Feb. 5,1996).
31. **Grolmes, M. A.,** "Pressure Relief Requirements for Organic Peroxide and Other Related Components," *Proc. Int. Symp. on Runaway Reactions, Pressure Relief Design, and Effluent Handling*, New Orleans (Mar. 11–13, 1998).
32. **Etchells, J. C., *et al.*,** "Relief System Sizing for Exothermic Runaway: The UK HSE Strategy," *Proc. Int. Symp. on Runaway Reactions, Pressure Relief Design, and Effluent Handling*, New Orleans (Mar. 11-13, 1998).

Table 6. Comparison of $(\rho c/\lambda(M_{w,v}),^{1/2}$ values with water.

System	Formula	M_w	ρ, kg m^{-3}	c, J kg^{-1} K^{-1}	λ, J kg^{-1}	$\rho c/\lambda(M_{w,v})^{1/2}$
Water	H_2O	18	1,000	4,300	2.2×10^6	0.46
Styrene	C_8H_8	104	793	2,023	3.52×10^5	0.45
Ethylbenzene	C_8H_{10}	106	760	1,957	3.39×10^5	0.43
Propane	C_3H_8	44	584	2,135	4.27×10^5	0.44
Phenol/Formaldehyde-Water	—	18	1,100	2,930	2.2×10^6	0.35
Propionic Anhydride	$C_6H_{10}O_3$	130	847	2,113	3.29×10^5	0.48
Isopropanol	C_3H_8O	60	723	3,109	6.64×10^5	0.44
Methanol	CH_4O	32	749	2,613	1.1×10^6	0.32
Acetic Anhydride	$C_4H_6O_3$	102	917	2,170	4.0×10^5	0.49

L/D = 100, C_D ~ 0.65; L/D = 200, C_D ~ 0.5; L/D = 400, C_D ~ 0.4, where L (m) is the equivalent pipe length and D (m) is the pipe dia.). Equations 14 and 15 result from Eqs. 9 and 10, representing the vapor system behavior by using relevant water properties and the gassy system behavior by considering a value of $M_{w,g}$ of 44 together with relevant calorimeter-specific parameters (v = 3.5 × 10^{-4} m^3 and m_t = 0.01 kg) for two DIERS-based units (RSST and ARSST).

This simple methodology has been benchmarked against available reactive large-scale data, including foamy (phenolic resins *(27)*, phenol/formaldehyde *(28)*, low-conversion ethylbenzene/styrene *(1)*), and nonfoamy (such as high-conversion ethylbenzene/styrene *(1)*, methanol/acetic anhydride *(26)*, and isopropanol/propionic anhydride *(32)* -like vapor systems), gassy systems (such as trimethyl hexanoyl peroxide and *t*-butyl peroxy benzoate *(29)* and dicumyl peroxide *(30)*), and hybrid systems (such as 50% hydrogen peroxide *(20)*).

Representative experimental data and comparisons with the screening guidelines are illustrated in Table 5. Nonreactive foamy systems such as the foamy water data *(9)* are not in Table 5. Such systems require special two-phase flow considerations as discussed earlier. This is because the noted overpressure effect in reducing the vent requirement for reactive vapor systems experiencing two-phase venting does not apply for foamy nonreactive systems.

Note especially that realistic vent sizes are provided by Eqs. 14 and 15 without having to specify any thermophysical properties, which are often not readily available. This is not surprising, considering that the value of the controlling property group $\rho c/\lambda(M_{w,v})^{1/2}$ in Eqs. 9 and 10 based upon water properties is similar to or envelopes most systems of interest (see Table 6).

Also, note again from Table 4 that if a vapor system can be shown to exhibit nonfoamy-like behavior, the vent area requirement can be reduced by a factor of about 2. The flow regime detector, as noted earlier, can distinguish between foamy and nonfoamy runaway conditions, in addition to determining relevant parameters such as vapor, gassy, or hybrid system behavior, and corresponding values of $\dot{T}$ and $\dot{P}$.

To sum up

A simple, cost-effective approach to relief system sizing has been outlined using the DIERS-based calorimetry methodology data. The data, which can be scaled directly to full-size applications, have been shown to produce excellent agreement with a large number of large-scale venting tests including vapor, hybrid, and gassy systems. Easy-to-use screening guidelines are provided for these systems, which eliminates the need for a detailed knowledge of thermophysical properties that are often not readily available for reactive chemical systems. CEP

H. K. FAUSKE is president of Fauske & Associates, Inc., Burr Ridge, IL ((630) 887-5200; Fax: (630) 986-5481; E-mail: Fauske@Fauske.com; Web Site: www.Fauske.com). Since leaving Argonne National Laboratory in 1980, where he was the first director of the Fast Reactor Safety Technology Management Center and was responsible for the planning and management of the DOE program, he has been involved in a wide range of safety issues, including providing overall technical direction for the DIERS development programs. Currently, he is involved in resolving potential safety issues concerned with waste storage tanks and the development of inherently safer nuclear and chemical-process reactor concepts. The author of over 200 articles, he holds numerous patents and is on the editorial boards of the *Journal of the Loss Prevention Industries* and the *International Journal of Multi-Phase Flow.* He has taught at several universities in the U.S. and abroad, and has served as the BASF Renowned Scientist Lecturer from 1989 to 1990. Fauske holds a DSc in chemical engineering from the Norwegian Institute of Technology, and is a fellow of the American Nuclear Society (ANS) and AIChE. His awards include the University of Chicago Medal for Distinguished Performance at Argonne National Laboratory, the Tommy Thompson Award given by ANS, and the Donald Q. Kern Award and Robert E. Wilson Award in Nuclear Chemical Engineering, both bestowed by AIChE.